

# Carborane Complexes of Ruthenium(III): Studies on Thermal Reaction Chemistry and the Catalyst Design for Atom Transfer Radical Polymerization of Methyl Methacrylate

Ivan D. Grishin,<sup>†</sup> Dmitrii I. D'yachihin,<sup>‡</sup> Alexander V. Piskunov,<sup>§</sup> Fedor M. Dolgushin,<sup>‡</sup> Alexander F. Smol'yakov,<sup>‡</sup> Mikhail M. Il'in,<sup>‡</sup> Vadim A. Davankov,<sup>‡</sup> Igor T. Chizhevsky,<sup>\*,‡</sup> and Dmitry F. Grishin<sup>\*,†</sup>

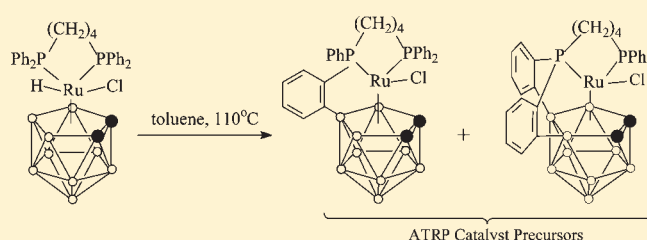
<sup>†</sup>Research Institute of Chemistry of the N. I. Lobachevsky Nizhny Novgorod State University, 23 Gagarin Avenue, Building 5, 603950 Nizhny Novgorod, Russian Federation

<sup>‡</sup>A. N. Nesmeyanov Institute of Organoelement Compounds of the RAS, 28 Vavilov Street, 119991 Moscow, Russian Federation

<sup>§</sup>G. A. Razuvaev Institute of Organometallic Chemistry of the RAS, 49 Tropinin Street, 603950 Nizhny Novgorod, Russian Federation

## Supporting Information

**ABSTRACT:** The heating of the 18-electron complex [3,3-(dppb)-3-H-3-Cl-*closo*-3,1,2-RuC<sub>2</sub>B<sub>9</sub>H<sub>11</sub>] (3) in benzene at 80 °C in the presence of a small amount of CCl<sub>4</sub> as initiator afforded paramagnetic 17-electron species [3,3-(dppb)-3-Cl-*closo*-3,1,2-RuC<sub>2</sub>B<sub>9</sub>H<sub>11</sub>] (4) along with minor amounts of two P-phenylene *ortho*-cycloboronated derivatives [3-Cl-3,3,8-{Ph<sub>2</sub>P(CH<sub>2</sub>)<sub>4</sub>PPh- $\mu$ -(C<sub>6</sub>H<sub>4</sub>-*ortho*)}-*closo*-3,1,2-RuC<sub>2</sub>B<sub>9</sub>H<sub>10</sub>] (5) and [3,7-Cl<sub>2</sub>-3,3,8-



{Ph<sub>2</sub>P(CH<sub>2</sub>)<sub>4</sub>PPh- $\mu$ -(C<sub>6</sub>H<sub>4</sub>-*ortho*)}-*closo*-3,1,2-RuC<sub>2</sub>B<sub>9</sub>H<sub>10</sub>] (6) in total yield of ca. 80%. The heating of either 3 or 4 in toluene at 95 °C in the absence of CCl<sub>4</sub> led to the selective formation of 5, which was isolated in 64% and 46% yield, respectively. Thermolysis of 3 at higher temperatures (boiling toluene, 110 °C) gives novel paramagnetic species [3-Cl-3,3,7,8-

{Ph<sub>2</sub>P(CH<sub>2</sub>)<sub>4</sub>P- $\mu$ -(C<sub>6</sub>H<sub>4</sub>-*ortho*)<sub>2</sub>}-*closo*-3,1,2-RuC<sub>2</sub>B<sub>9</sub>H<sub>9</sub>] (7) featuring bis(*ortho*-cycloboronation) of both P-phenyl groups at the same phosphorus atom of the ruthenium-bound dppb ligand. All new paramagnetic complexes 4–7, as well as starting diamagnetic species 3, were characterized by single-crystal X-ray diffraction and, in addition, by EPR spectroscopic studies of odd-electron complexes. Ruthenacarboranes 3–5 and 7 all display high efficiency as catalysts for the atom transfer radical polymerization (ATRP) of methyl methacrylate (MMA). Complex 5 gave the best catalyst performance in terms of polydispersity; the PDI ( $M_w/M_n$ ) of the polymer samples is as low as 1.15.

## INTRODUCTION

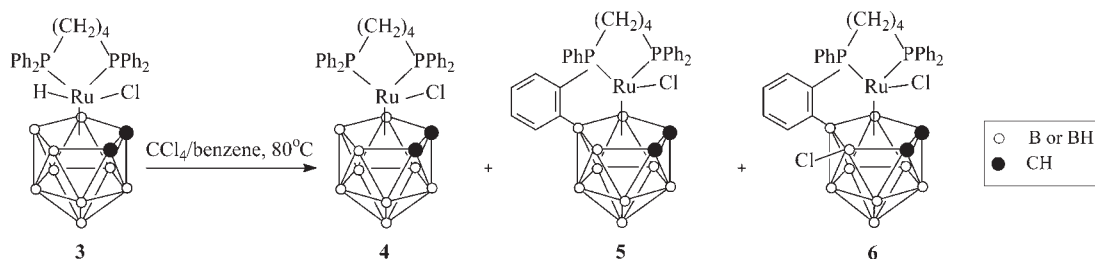
Ruthenium complexes combined with different Lewis-acid-type activators or in the absence of additives have found use as catalyst precursors in radical processes derived from Kharasch chemistry,<sup>1</sup> such as the atom transfer radical polymerization (ATRP) of vinyl monomers,<sup>2</sup> which is commonly referred to as the “living” polymerization.<sup>2a</sup> Mononuclear half-sandwich ruthenium(II) complexes with cyclopentadienyl or arene ligands such as [RuCp(PPh<sub>3</sub>)<sub>2</sub>Cl],<sup>3a–d</sup> [RuCp\*(PPh<sub>3</sub>)<sub>2</sub>Cl],<sup>3b–d</sup> [RuCp\*(PCy<sub>3</sub>)Cl],<sup>3c</sup> [RuInd(PPh<sub>3</sub>)<sub>2</sub>Cl],<sup>3a,b,d</sup> [RuCl<sub>2</sub>(*p*-cymene)(L)] (L = PR<sub>3</sub><sup>3e,f</sup> or N-heterocyclic carbenes<sup>3g,h</sup>) and their homo- and heterobimetallic derivatives,<sup>3i</sup> RuCl<sub>2</sub>(PPh<sub>3</sub>)<sub>3</sub>,<sup>3j,k</sup> Grubbs’ ruthenium–carbene complex RuCl<sub>2</sub>(=CHPh)-(PCy<sub>3</sub>)<sub>2</sub>,<sup>3e,f,l</sup> as well as *closo*- and *exo-nido*-ruthenacarboranes of different types and structures<sup>3d,m,n</sup> are examples of ruthenium-based ATRP catalysts extensively investigated in recent years. It is believed that in terms of steric and electronic properties dianionic dicarbollide ligands, such as [7,8-*nido*-C<sub>2</sub>B<sub>9</sub>H<sub>11</sub>]<sup>2-</sup> and

its derivatives, can serve as models of  $\eta^5$ -alkylcyclopentadienyl ligands and, in particular, of the  $\eta^5$ -pentamethylcyclopentadienyl (Cp\*) ligand.<sup>4a–c</sup> However, due to the doubly negative charge, the carborane ligands much better stabilize complexes containing metals in higher oxidation state.<sup>4d,e</sup> Thus, the stable seven-coordinate Ru(IV) compounds [3,3-(Ph<sub>3</sub>P)<sub>2</sub>-3-H-3-(L)-*closo*-3,1,2-RuC<sub>2</sub>B<sub>9</sub>H<sub>11</sub>] (1, L = Cl; 2, L = H) belonging to the family of 18-electron *closo*-ruthenacarboranes have been described.<sup>5</sup> An analogue of complex 1 with the chelating diphosphine ligand [3,3-(dppb)-3-H-3-Cl-*closo*-3,1,2-RuC<sub>2</sub>B<sub>9</sub>H<sub>11</sub>] (3) also belongs to this family. The latter 18-electron complex has only recently become conveniently available by the exploitation of the phosphine–diphosphine displacement reaction of either *closo* complex 1<sup>5d</sup> or its *exo-nido* isomer.<sup>6</sup> *closo*-Ruthenacarboranes,

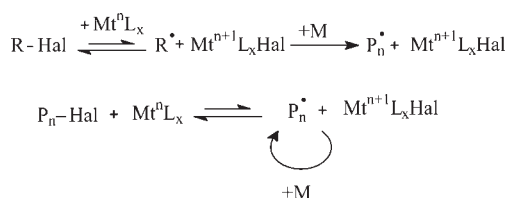
Received: March 9, 2011

Published: July 11, 2011

Scheme 1



such as **1** and **3**, are of interest not only due to the fact that they belong to structurally rare examples of seven-coordinate Ru(IV) complexes but also due to their unprecedented use as efficient catalysts for atom transfer radical polymerization (ATRP): a convenient way toward well-defined polymers based on vinyl monomers.<sup>5d,7</sup> The general scheme for ATRP process can be described by the following scheme:



Here,  $\text{Mt}^n\text{L}_x$  indicates a complex based on a transition metal  $\text{Mt}$ ,  $n$  is the oxidation state of the metal atom,  $\text{L}$  represents the auxiliary ligands,  $\text{R-Hal}$  is the organohalide initiator ( $\text{Hal} = \text{Cl}$  or  $\text{Br}$ ), and  $\text{P}_n$  is the propagating polymer chain. The polymerization starts from generation of radical species via reversible activation of a terminal carbon-halogen bond in organohalide compound and its addition to monomer unit ( $\text{M}$ ). The equilibrium between active and dormant species leads to the step-by-step growth of the polymer chains leading to polymers with narrow polydispersity.

In accord with our preliminary communication,<sup>8</sup> we report here our studies on thermal reactions of the diamagnetic complex **3**<sup>6</sup> in the presence and in the absence of  $\text{CCl}_4$  as initiator. By employing these general routes, we have substantially extended the scope of the known paramagnetic Ru(III) *closo*-ruthenacarborane complexes, some of which were found to exhibit high efficiency as ATRP catalysts to controlled polymerization of MMA.

## RESULTS AND DISCUSSION

**Synthesis of *closo*-Ruthenacarboranes (4–7) and Examination of Their Thermal Reactions in the Presence and in the Absence of  $\text{CCl}_4$  as a Source of Radicals.** The previous studies have shown that in the presence of  $\text{CCl}_4$  *closo*-ruthenacarboranes **1** and **3** can efficiently initiate the ATRP polymerization of MMA and styrene<sup>7,8</sup> in the absence of additional activators. However, the above-mentioned diamagnetic Ru(IV) complexes are coordinatively and electronically saturated compounds and, in terms of catalytic activity of organometallic ATRP catalysts,<sup>2a</sup> cannot be considered as true catalysts for this process. Taking into account the fact that the polymerization of MMA or styrene in the presence of complexes **1** and **3** occurs in bulk at relatively high temperatures (80 °C and higher), in the work that we now report, we investigated in detail the thermal reactivity of

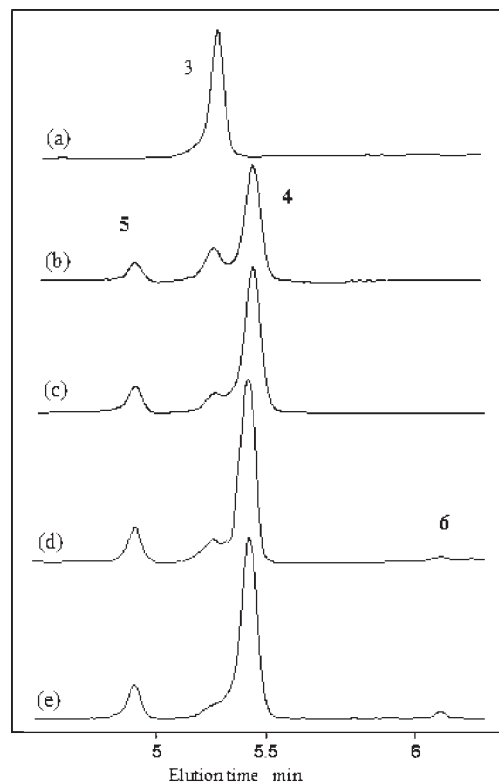


**Figure 1.** The HPLC monitoring of the reaction of diamagnetic complex **3** in benzene solution in the presence of  $\text{CCl}_4$  at 80 °C. The reaction time: (a) 0 h, (b) 1 h, (c) 2 h, (d) 3 h, (e) 4 h.

complex **3** in benzene and toluene at different temperatures in the presence and in the absence of traces of  $\text{CCl}_4$ .

Diamagnetic *closo*-ruthenacarborane **3** is known to be quite stable both in the solid state and in solution.<sup>6</sup> It also remains intact after heating in benzene under reflux for about 15–17 h. However, when a benzene solution of **3** was heated under the same thermal conditions in the presence of traces of  $\text{CCl}_4$ , three new ruthenacarboranes (**4–6**) were obtained, among which **4** was the major product (Scheme 1). The TLC monitoring of this reaction did not give a clear control of the reaction due to very close  $R_f$  values for complexes **3**, **4**, and **5**. In addition, all three products **4–6** are paramagnetic, which complicates their identification by  $^1\text{H}$  and/or  $^{31}\text{P}\{^1\text{H}\}$  NMR spectroscopy. In an attempt to control the reaction, we tried to apply HPLC on Separon SGX column using  $\text{CH}_2\text{Cl}_2/n$ -hexane (1:3) as mobile phase. On the basis of the HPLC data obtained (Figure 1), we not only accurately estimated the relative ratio of the final products

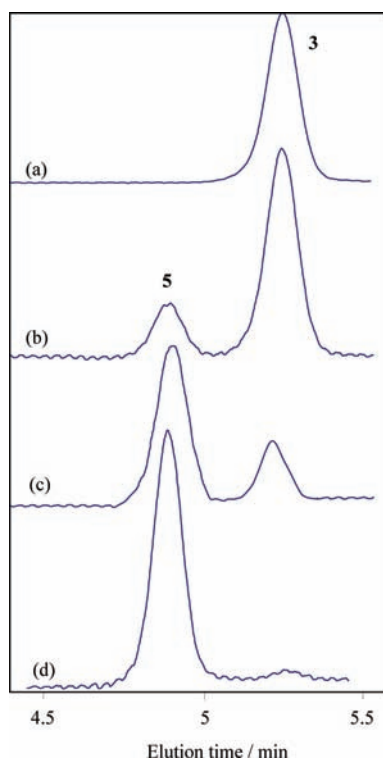


**Figure 2.** HPLC monitoring of the thermolysis of **3** in toluene solution at 95 °C. The reaction time: (a) 0 h, (b) 1 h, (c) 4 h, (d) 7 h.

**4**, **5**, and **6** as 5:1:0.1 but also determined the time of complete conversion of diamagnetic complex **3** (ca. 4 h). As can be seen from Figure 1, an increase in the degree of conversion of starting complex **3** is not accompanied by the accumulation of complex **5** due to the consumption of the major reaction product **4**. Complex **5** seems to be generated from the starting diamagnetic complex **3** rather than from complex **4** during this thermal reaction. It should also be noted that product **6** apparently appeared in later steps of the reaction, most probably from complex **5**.

The reaction of **3** with  $\text{CCl}_4$  can occur in benzene even at lower temperature (60 °C). However, under these conditions the reaction proceeds slower affording complexes **4** and **5** in a ratio of ca. 6:1, and the conversion of **3** achieved after 6 h was less than 50% (HPLC data).

The main paramagnetic complex **4** was always accompanied by species **5** during its synthesis and isolation. The best yield (21%) of compound **4** containing **5** in a 10:1 ratio was obtained by treatment of the crude reaction mixture with the preparative column chromatography on silica gel followed by 3-fold recrystallization from a  $\text{CH}_2\text{Cl}_2/n$ -hexane mixture. However, some amount of **4** in HPLC pure form could ultimately be obtained by additional recrystallization of the residual obtained from the combined mother liquors (see Experimental Section). The other two complexes **5** and **6** were in turn individually prepared in moderate yield by alternative methods starting from **3** and **5**, respectively (vide infra). On the basis of the X-ray crystal data, complexes **4**–**6** were finally formulated as  $[\text{3,3-(dppb)-3-Cl-closo-3,1,2-RuC}_2\text{B}_9\text{H}_{11}]$ , **4** (major product) and its two *ortho*-phenylenecycloboronated derivatives  $[\text{3-Cl-3,3,8-}\{\text{Ph}_2\text{P}(\text{CH}_2)_4\text{-PPh-}\mu\text{-(ortho-C}_6\text{H}_4)\}\text{-closo-3,1,2-RuC}_2\text{B}_9\text{H}_{10}]$ , **5**, and  $[\text{3,7-Cl}_2\text{-3,3,8-}\{\text{Ph}_2\text{P}(\text{CH}_2)_4\text{PPh-}\mu\text{-(ortho-C}_6\text{H}_4)\}\text{-closo-3,1,2-RuC}_2\text{B}_9\text{H}_{10}]$ , **6**.

**Scheme 2**

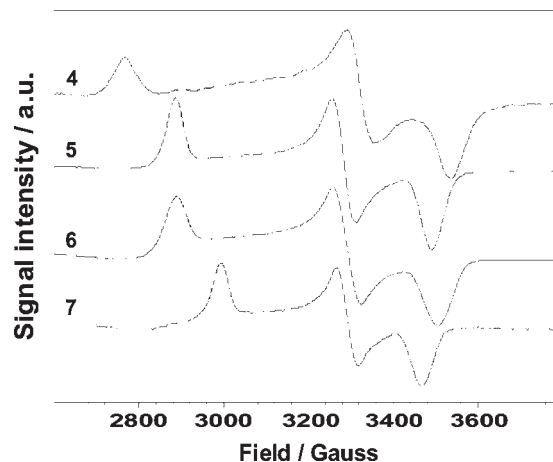
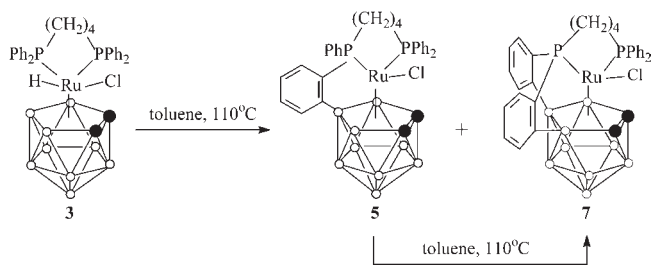


**Figure 3.** Anisotropic EPR spectra of ruthenacarboranes **4**–**7** recorded in a  $\text{CH}_2\text{Cl}_2$ /toluene mixture at 150 K.

Interestingly, although complex **3** is thermally inert in a benzene solution at 80 °C, under more forcing conditions (heating in a toluene solution at 95 °C) this compound produced selectively *ortho*-phenylenecycloboronated paramagnetic complex **5** in 64% yield. The HPLC monitoring of the reaction (Figure 2) showed that complex **5** is the only reaction product, and the formation of complex **4** was not observed under these conditions. Attempts to convert complex **4** into **5** by its thermal treatment under the same condition as for **3** resulted in the formation of the desired product in 46% yield. It should also be noted that under anaerobic conditions complex **5** reacted with the chlorinated solvent  $\text{CCl}_4$  under gentle reflux affording chloro-cage substituted complex **6** in 68% yield. Each of these complexes **5** and **6** has been isolated as an air-stable crystalline solid by the preparative column chromatography on silica gel and characterized by a combination of analytical and EPR spectroscopic data, including their single crystal X-ray diffraction studies.

We next examined the thermolysis of **3** in toluene under more drastic thermal conditions at 110 °C. This reaction unexpectedly afforded, along with **5**, the paramagnetic complex  $[\text{3-Cl-3,3,}$

$\text{7,8-}\{\text{Ph}_2\text{P}(\text{CH}_2)_4\text{P(ortho-C}_6\text{H}_4)_2\}\text{-closo-3,1,2-RuC}_2\text{B}_9\text{H}_9]$  (**7**) (Scheme 2). The structure of **7** was deduced from the X-ray diffraction data (vide infra). From these data it follows that although **7** has a polyhedral structure similar to that of **5**, it exhibits bis(*ortho*-cycloboronation) of two P-phenyl groups connected with the same phosphorus atom of the ruthenium-bound dppb ligand. In contrast to a number of known monocarbon<sup>9</sup> and dicarbon metallacarboranes,<sup>7a,10</sup> as well

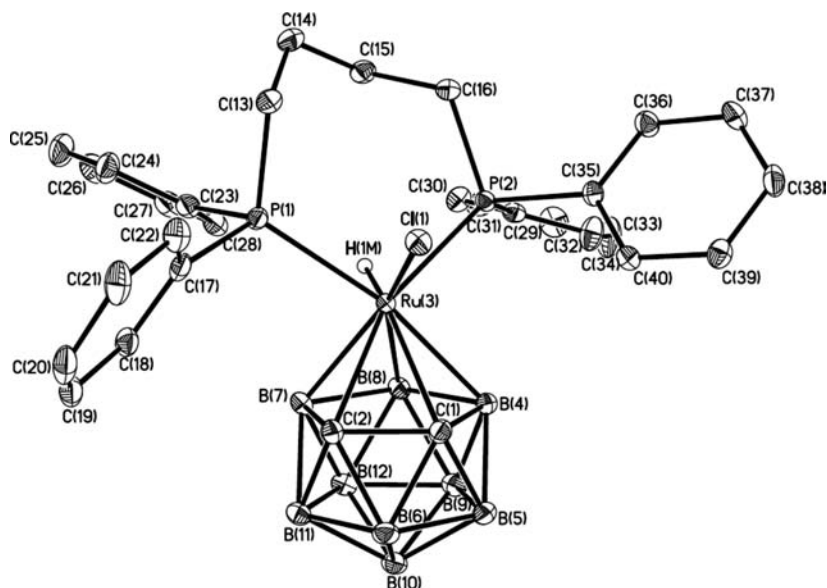


**Figure 4.** ORTEP representation of the molecular structure with the numbering scheme for diamagnetic complex **3**; ellipsoids are drawn at the 50% probability level (all hydrogen atoms excluding ruthenium–hydride are omitted for clarity). Selected bond lengths (Å) and angles (deg): Ru(3)–C(1) 2.258(2), Ru(3)–C(2) 2.229(2), Ru(3)–B(4) 2.315(2), Ru(3)–B(7) 2.230(2), Ru(3)–B(8) 2.282(2), Ru(3)–P(1) 2.3670(5), Ru(3)–P(2) 2.3305(5), Ru(3)–Cl(1) 2.4463(5), Ru(3)–H(1M) 1.51(3), C(1)–C(2) 1.624(3); P(1)–Ru(3)–P(2) 102.51(2), P(1)–Ru(3)–Cl(1) 80.48(2), P(2)–Ru(3)–Cl(1) 83.12(2), Cl(1)–Ru(3)–H(1M) 136(1).

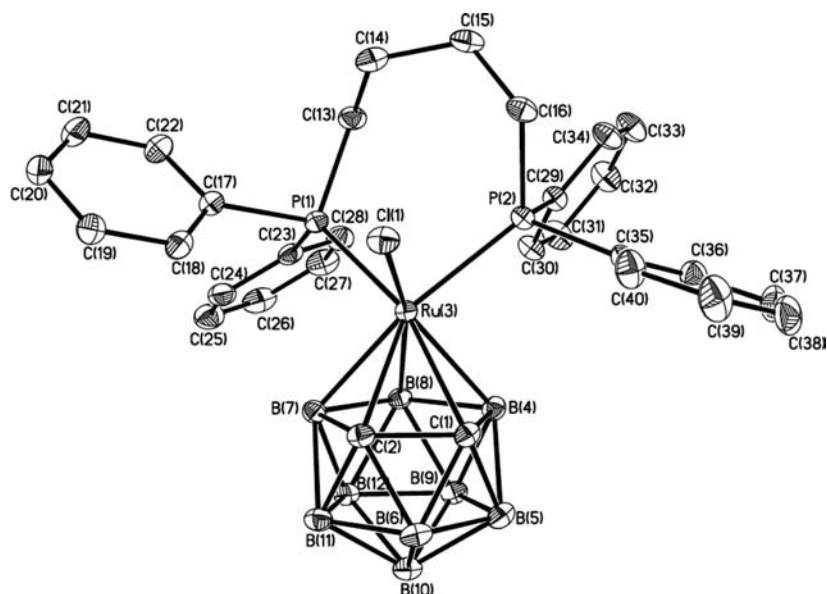


**Figure 5.** ORTEP representation of the molecular structure with the numbering scheme for complex **4**; ellipsoids are drawn at the 50% probability level (all hydrogen atoms are omitted for clarity).

as metallaborane clusters<sup>11</sup> with an *exo*-cyclic linkage induced by *ortho*-cycloboronation of one of the P-phenyl rings of the metal-bound monophosphine or diphosphine ligands, complex **7** containing two “one-site” *ortho*-phenylenecycloboronated linkages represents a novel type of 12-vertex *closo*-metallacarboranes belonging to this family (see the discussion in the following section).

It was then found that heating a solution of **5** in toluene at 110 °C also afforded complex **7**. However, in both cases, starting from **3** or **5**, complex **7** is formed in moderate yield due to its

partial decomposition during thermal treating and isolation. Thus, the heating of compound **5** under reflux in toluene for 14 h afforded **7** in a yield of at most 35%. These observations suggest that the thermal reaction of **3** under these conditions (toluene, 110 °C) occurs stepwise to give the final product **7** through the intermediate formation of complex **5**.

The paramagnetic nature of complexes **4**–**7** was further confirmed by EPR spectroscopy. As expected, the spectra of all four complexes proved to be similar in that they exhibit rhombic g component patterns with  $g_1 = 2.487$ ,  $g_2 = 2.070$ ,  $g_3 = 1.947$  for

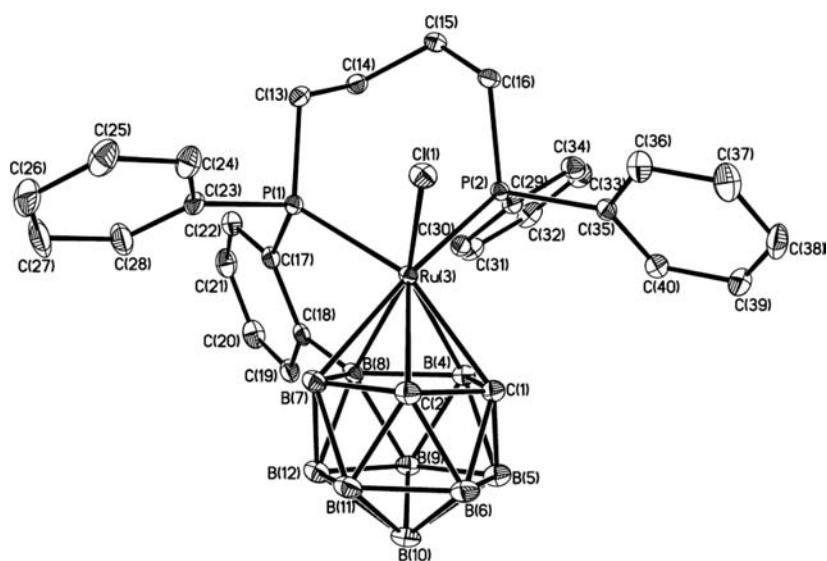


**Figure 6.** ORTEP representation of the molecular structure with the numbering scheme for complex 5; ellipsoids are drawn at the 50% probability level (all hydrogen atoms are omitted for clarity).

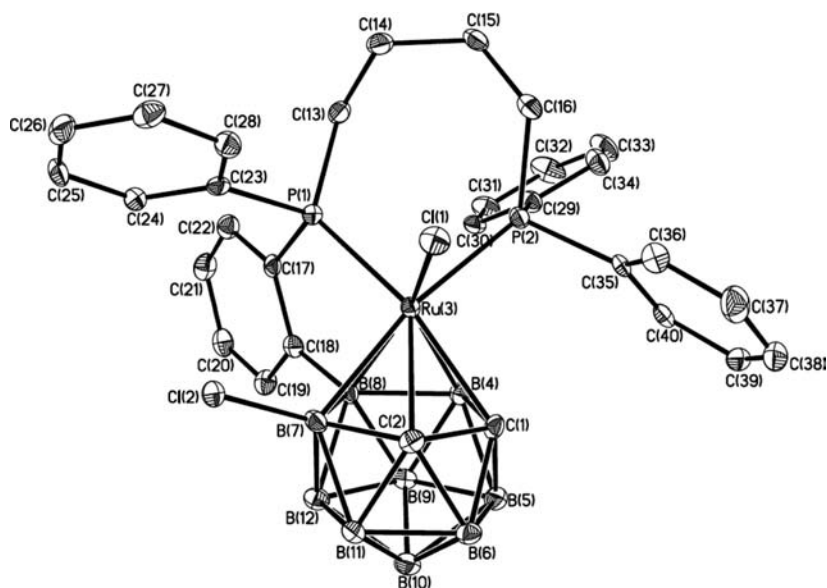


**Figure 7.** ORTEP representation of the molecular structure with the numbering scheme for complex 6; ellipsoids are drawn at the 50% probability level (all hydrogen atoms are omitted for clarity).

4;  $g_1 = 2.385$ ,  $g_2 = 2.095$ ,  $g_3 = 1.972$  for 5;  $g_1 = 2.384$ ,  $g_2 = 2.091$ ,  $g_3 = 1.965$  for 6; and  $g_1 = 2.300$ ,  $g_2 = 2.091$ ,  $g_3 = 1.986$  for 7. The anisotropic spectra in a toluene–methylene chloride mixture as the solid matrix are shown in Figure 3. The EPR spectra of complexes 4–7 are similar to the spectra of other ruthenium complexes containing the metal atom in a pseudo-octahedral coordination.<sup>6,10,12</sup> A comparison of these spectra shows that the presence of one or two *ortho*-cycloboronated moieties in these compounds leads to a gradual shift of the first component of the signal to a higher field, whereas the positions of two other components vary only slightly. It is interesting that the EPR spectra of compounds 5 and 6 are virtually identical, which may indicate that the chlorine atom bound to the carborane moiety is not involved in the delocalization of the unpaired electron.

**Single-crystal X-ray Diffraction Studies of Diamagnetic and Paramagnetic Complexes 3–7.** The structure of diamagnetic complex 3 has been previously determined by a combination of analytical and multinuclear NMR spectroscopic data,<sup>6</sup> and in the present work it was unambiguously confirmed by X-ray crystallography. Figure 4 depicts the molecular structure of 3 with selected bond lengths and angles. Complex 3 belongs to a group of neutral seven-coordinate Ru(IV) complexes.<sup>5</sup> The ruthenium atom in 3 is quite symmetrically  $\eta^5$ -coordinated by the *nido*- $\{C_2B_9\}$  cage ligand, so that the Ru–C(1,2) (2.2582(19) and 2.229(2) Å) and Ru–B(4,7,8) (2.282(2)–2.315(2) Å) distances are approximately equal and are consistent with those in structurally similar complex 1.<sup>5d</sup> Two terminal chlorine (Ru–Cl, 2.4463(5) Å) and hydrido (Ru–H, 1.51(3) Å) ligands,

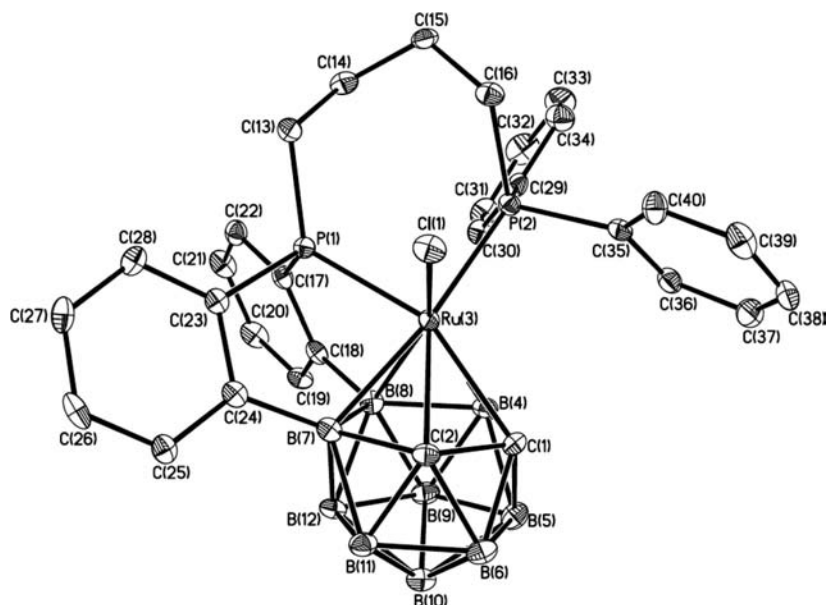


**Figure 8.** ORTEP representation of the molecular structure with the numbering scheme for one of two independent molecules of complex **7**; ellipsoids are drawn at the 50% probability level (all hydrogen atoms are omitted for clarity).

along with one chelating dppb ligand (Ru–P(1,2), 2.3670(5) and 2.3305(5) Å), in sum occupy four coordination sites, completing the seven-coordinate geometry at the Ru(IV) center. The arrangement of the metal-bound H, Cl, and dppb ligands with respect to the open face of the cage ligand in **3** is typical of seven-coordinate Ru(IV) *closo*-metalacarboranes containing the {RuClHP<sub>2</sub>} vertex. As in related complex **1**,<sup>5d</sup> the position of these ligands is such that the Ru–H bond in **3** is projected onto the B(8)–H bond (the H(3)–Ru–B(8)–H(8) torsion angle is 19°), and there is a very short H(8)···H(3) (2.20 Å) distance, which is indicative of the possible through-space interaction between these two hydrogen atoms. This is also evidenced by the unique H<sub>Ru</sub>···H<sub>B(8)}</sub> coupling with <sup>3</sup>J(H,H) = 6.0 Hz in the <sup>1</sup>H NMR spectrum of complex **3**, which is comparable with the <sup>3</sup>J(H<sup>Ru</sup>,H<sup>B</sup>) coupling in the spectra of other structurally similar *closo*-ruthenacarboranes **1**<sup>5d</sup> (10.3 Hz) and [2-Cl-2-H-2,5-(Ph<sub>3</sub>P)<sub>2</sub>-3,9-(MeO)<sub>2</sub>-2,1-RuCB<sub>8</sub>H<sub>6</sub>] (**8**)<sup>13</sup> (9.6 Hz).

The structures of paramagnetic complexes **4**–**7** in the solid state were also determined by X-ray diffraction studies, which unambiguously confirmed their 17-electron *closo* structures. The molecular structures of **4**–**7** are shown in Figures 5–8, respectively, and their selected geometrical parameters (bond distances and angles) are listed in Table 1. As expected, the ruthenium atom in all these complexes has the coordination number of six being formally a three-valent 17-electron metal center. In all complexes **4**–**7**, the metal atom is coordinated by one chlorine atom and two phosphorus atoms of the chelating dppb ligand and, in addition, is bound in a η<sup>5</sup>-fashion to the C<sub>2</sub>B<sub>3</sub> open face of the carborene cage ligand, with the ruthenium-to-cage-atom distances being approximately the same in paramagnetic complex **4** and species **5**–**7** which have *ortho*-phenylcycloboronated linkages (Table 1). Moreover, the latter distances are very similar to those observed in a number of known electronically saturated *closo*-ruthenacarboranes with a similar ligand arrangement at the metal vertex, including complex **3** (except for a somewhat elongated Ru–B(4) distance equal to 2.315(2) Å). At the same time, the Ru–Cl bond lengths in **4**–**7** (2.3681(6)–2.3853(8) Å)

**Table 1.** Selected Bond Lengths (Å) and Angles (deg) for Paramagnetic Complexes **4**–**6** and for Two Independent Molecules of **7** (A and B)

	7				
	4	5	6	A	B
Bond Lengths (Å)					
Ru(3)–C(2)	2.217(2)	2.237(3)	2.245(3)	2.203(3)	2.208(3)
Ru(3)–C(1)	2.249(2)	2.270(3)	2.248(3)	2.262(3)	2.254(3)
Ru(3)–B(4)	2.250(2)	2.228(3)	2.227(3)	2.232(4)	2.246(4)
Ru(3)–B(7)	2.240(2)	2.243(3)	2.280(4)	2.230(4)	2.239(4)
Ru(3)–B(8)	2.274(2)	2.254(3)	2.281(3)	2.247(4)	2.256(4)
Ru(3)–P(1)	2.3531(5)	2.3000(7)	2.3127(9)	2.2692(9)	2.2689(9)
Ru(3)–P(2)	2.3784(5)	2.3739(7)	2.3693(9)	2.3556(9)	2.3423(9)
Ru(3)–Cl(1)	2.3710(5)	2.3681(6)	2.3699(9)	2.3853(8)	2.3723(9)
C(1)–C(2)	1.617(3)	1.600(4)	1.592(4)	1.620(4)	1.632(5)
C(18)–B(8)		1.590(4)	1.582(4)	1.591(5)	1.571(5)
C(24)–B(7)				1.596(5)	1.580(5)
Bond Angles (deg)					
P(1)–Ru(3)–P(2)	92.06(2)	92.28(2)	89.45(3)	89.93(3)	91.27(3)
P(1)–Ru(3)–Cl(1)	94.53(2)	91.93(2)	100.43(3)	89.52(3)	87.37(3)
P(2)–Ru(3)–Cl(1)	87.37(2)	92.28(2)	87.15(3)	90.78(3)	91.21(3)

are much shorter than those found in 18-electron anionic chloro-containing complexes, such as [Et<sub>4</sub>N][3-Cl-3,3-(PPh<sub>3</sub>)<sub>2</sub>-*closo*-3,1,2-RuC<sub>2</sub>B<sub>9</sub>H<sub>11</sub>] [2.515(2) Å]<sup>14</sup> and [Au(PPh<sub>3</sub>)<sub>2</sub>][3-Cl-3,3-(CO)<sub>2</sub>-*closo*-3,1,2-RuC<sub>2</sub>B<sub>9</sub>H<sub>11</sub>] [2.452(1) Å],<sup>15</sup> as well as in neutral *closo*-ruthenacarboranes like complex **1** [2.4284(5) Å].<sup>5d</sup> The X-ray diffraction study showed that complex **6** contains two chlorine atoms, of which one is terminal with respect to the metal atom, whereas another chlorine atom is bound to the cage B(7) atom [B(7)–Cl, 1.803(4) Å] (Figure 7). Another particularly interesting structural feature of complexes **5**–**7** is that either one

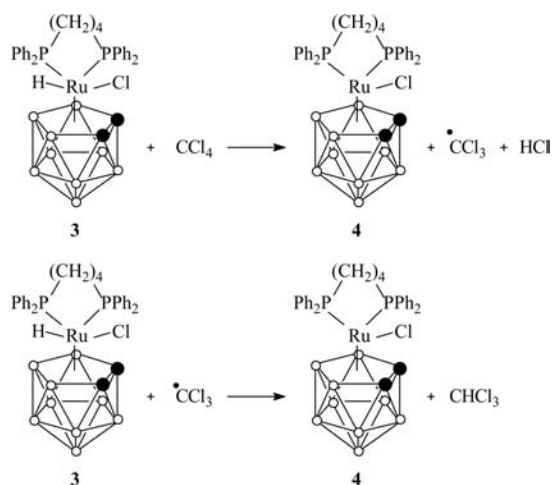
or two P-phenyl rings of the ruthenium-bound diphosphine ligand are *ortho*-cycloboronated to the cluster boron atoms adjacent to ruthenium. As mentioned above, complexes **5** and **6** exhibit mono-*ortho*-cycloboronation, whereas complex **7** displays bis- (*ortho*-cycloboronation) of two phenyl groups bound to the same phosphorus atom of the dppb ligand. As far as we are aware, only two other structurally characterized boron-containing clusters exhibiting double *ortho*-cycloboronation of P-phenyl groups are known in the literature. One cluster belongs to the monocarbon *arachno* 10-vertex

platinacarborane clusters,  $[(\text{Ph}_2\text{P-ortho-C}_6\text{H}_4)_2\text{PtCB}_8\text{H}_{10}]$ ,<sup>16</sup> and another one belongs to *closo* six-vertex diiridohexaboranes,

$[(\text{CO})_3(\text{PPh}_3)(\text{Ph}_2\text{P-ortho-C}_6\text{H}_4)_2(\text{Ir}_2\text{B}_4\text{H}_2)]$ .<sup>17</sup> In both species, the bis(*ortho*-cycloboronated) linkages associated with different P-phenyl groups of the metal-bound monophosphine ligands. It should be noted that there are two independent molecules of complex **7** which show only small differences in their bond distances and angles (Table 1). The molecular structure of only one independent molecule is therefore shown in Figure 8.

**Mechanistic Aspects of Conversion of Diamagnetic Complex **3** into *closo*-Ruthenacarboranes **4** and **5** under Thermal/ $\text{CCl}_4$  Conditions.** The formation of 17-electron species **4** from diamagnetic complex **3** in the presence of  $\text{CCl}_4$  was unexpected. The pathway by which **3** forms paramagnetic complex **4** may be described by the two-step reaction of **3** with  $\text{CCl}_4$  as shown in Scheme 3. The terminal H ligand at the Ru(IV) center of complex **3** can be activated by the intramolecular interaction with the boron hydride located at the eighth position

Scheme 3



of the carborane cage ligand before being detached to give HCl. As mentioned above, this interaction is confirmed by the geometry of **3** found in the solid-state structure (Figure 1), as well as by the unique long-range  $\text{H}^{\text{Ru}} \cdots \text{H}^{\text{B}(8)}$  coupling with  $J(\text{H},\text{H}) = 6.0$  Hz observed in the  $^1\text{H}$  NMR spectrum of **3**,<sup>6</sup> which we believe to occur via the through-space spin–spin coupling between these two hydrogen atoms. As a result, both the corresponding paramagnetic species **4** and the  $\text{CCl}_3^\bullet$  radical are formed, and the latter could also function as a hydrogen-abstracting reagent to form the next molecule of complex **4** (Scheme 3).

The formation of *ortho*-phenylcycloboronated complex **5** in the reaction of **3** in toluene at 95 °C in the absence of  $\text{CCl}_4$  as a source of radicals can proceed either by the thermal activation of **3** accompanied by the elimination of dihydrogen from *ortho*-phenyl C–H and the cage B–H moieties, as it has been observed for some other mono-*ortho*-phenylcycloboronated metallaborane complexes<sup>11e,f</sup> or via the mechanism proposed earlier by Stone and co-workers.<sup>9c</sup> In the latter case, the terminal hydrogen at the metal center in **3**, if it carries a positive charge, can protonate the hydride atom B(8)–H, which should have pronounced hydride properties due to the fact that the B(8) vertex is most distant from the electropositive cage carbon atoms. The next step may be viewed as the electrophilic substitution of the nearest dppb ligand Ph-ring at the *ortho* position by the naked B(8)<sup>+</sup> center which is formed after the elimination of  $\text{H}_2$ . Formation of B(8)–C(Ar)  $\sigma$ -bond with subsequent elimination of  $\text{H}^+$ , which in its turn abstracts one electron from the metal center, ultimately completes the transformation of **3** into **5**. The clean reaction and the high yield of **5** might suggest that a driving force for the *ortho*-cycloboronation occurring in this case is the conversion from sterically crowded (and hence more labile) Ru(IV) species to the more stable Ru(III) *closo*-ruthenacarborane.

**Quantum-Chemical Modeling of Reactions between Investigated Complexes.** It was found that the above *closo*-ruthenacarborane complexes with diphosphine ligands can undergo transformations either under thermal conditions or in the presence of free radicals in the reaction system to form in both cases stable paramagnetic species. To study the events of these reactions and to elucidate their possible mechanism, we performed the quantum chemical modeling of the processes lying at the basis of these transformations. Actually, we analyzed the conversion of complex **3** into **4** described by Scheme 3 as well as the reactions giving rise to *ortho*-phenylcycloboronated *closo*-ruthenacarboranes, namely the transformation of complex **4** into **5** and **5** into **7**, respectively, which are accompanied by the elimination of dihydrogen under relatively mild thermal conditions.

Table 2. Calculated Energy Changes in the Gas-Phase Reactions at 80 °C

reaction		calculation method					
		B3PW91/gen <sup>a</sup>			B3LYP/gen <sup>a</sup>		
		$\Delta_r E$ , kcal/mol	$\Delta_r H$ , kcal/mol	$\Delta_r G$ , kcal/mol	$\Delta_r E$ , kcal/mol	$\Delta_r H$ , kcal/mol	$\Delta_r G$ , kcal/mol
1	$3 + \text{CCl}_4 \rightarrow 4 + \text{HCl} + \text{CCl}_3^\bullet$	21	22	7.4	17	18	3.4
2	$3 + \text{CCl}_3^\bullet \rightarrow 4 + \text{CHCl}_3$	–31	–32	–32	–35	–35	–35
3	$4 \rightarrow 5 + \text{H}_2$	–8.4	–6.9	–15	–6.3	–4.8	–13
4	$5 \rightarrow 7 + \text{H}_2$	–1.5	0.2	–8.8	0.5	2.1	–6.7

<sup>a</sup>The composite basis set: 6-31G(d) for H, B, C, Cl, and P, and LanL2DZ + ECP for ruthenium.

To estimate the probability that the reactions proceed according to the suggested schemes, we carried out quantum-chemical calculations by the density functional theory (DFT) with the use of the B3LYP and B3PW91 functionals. We employed the composite basis set consisting of the 6-31G(d) basis set for period 1–3 elements and the LanL2DZ basis set including the effective core pseudopotential (ECP), which models the behavior of core electrons, for the ruthenium atom. The calculation method was chosen taking into account that it gives adequate and reliable results when modeling the structures of coordination ruthenium and other transition metal compounds.<sup>18</sup> The validity of the chosen model is confirmed by the good agreement between the bond lengths and bond angles calculated by the geometry optimization of the metal complexes and the above-considered results of the X-ray diffraction study. It was found that the best agreement of the geometrical parameters is achieved with the use of the B3PW91 functional. The calculations of the geometry of the complexes with the use of the B3LYP functional led to the larger bond lengths than those determined from the X-ray diffraction data. An analogous situation has been observed previously in the calculations of ruthenium complexes by this method.<sup>18d,e</sup>

Table 2 gives the energy, enthalpy, and free energy changes estimated by quantum chemical calculations. It should be noted that the calculations with the use of different functionals gave similar results and are, on the whole, in agreement with the experimental data.

**Table 3. Molecular-Weight Characteristics of polyMMA Obtained in the Presence of *closo*-Ruthenacarboranes 3–5 and 7 at 80 °C for 80 h**

complex	conversion	$M_n$	$M_w$	$M_w/M_n$	$M_{n, \text{theor}}$
3	80	19 100	23 100	1.21	30 400
4	66.8	18 800	21 900	1.17	25 300
5	58.4	15 700	18 000	1.15	22 200
7	62.4	14 700	17 000	1.16	23 700

The positive enthalpy and free energy changes for the reaction of complex 3 with  $\text{CCl}_4$  (line 1, Table 2) indicate that this process is endothermic and is favored by high temperature. This is confirmed by experimental data. As mentioned above, the reaction of complex 3 with  $\text{CCl}_4$  at 60 °C proceeds more slowly than at 80 °C. We suggest that this process can be represented by the two-step reaction according to Scheme 3 (see also lines 1 and 2, Table 2). Apparently, it is the step (1) giving  $\text{CCl}_3^\bullet$  radicals that is rate-limiting in this process. Step 2, which results in the abstraction of the hydrogen atom from 3 to form paramagnetic complex 4, is the energetically favorable process, as evidenced by the large negative free energy of this reaction.

The calculated energies for step 2 are indicative of the low kinetic stability of complex 3 in the presence of free radicals. It is necessary to take this fact into account in the analysis of the reactivity of complex 3 under the atom transfer radical polymerization conditions,<sup>7</sup> where it is gradually transformed into 4, and the resulting paramagnetic compounds are responsible for the polymerization, particularly at high degrees of conversion of the monomer (*vide infra*). On the whole, the negative free energies for steps 3 and 4 confirm that the formation of complexes with the mono-*ortho*-phenylenecycloboronated linkage is energetically favorable. However, the formation of the second *ortho*-cycloboronated linkage is energetically less favorable, as evidenced by more drastic conditions of the formation of complex 7 starting from mono-*ortho*-phenylenecycloboronated complex 5.

**Catalytic Activity of Complexes 3–5 and 7 in the Atom Transfer Radical Polymerization (ATRP) of Methyl Methacrylate (MMA).** Diamagnetic and paramagnetic *closo*-ruthenacarboranes 3–5 and 7 were examined as precatalysts for the controlled radical polymerization of MMA initiated by  $\text{CCl}_4$ . The results showing the molecular-weight characteristics of the final polymers are summarized in Table 3. A comparison of the polydispersity indexes of the samples shows that the polymers synthesized in the presence of paramagnetic complexes 4, 5, and 7 are smaller than that in the case of diamagnetic complex 3. This suggested that the paramagnetic complexes, which are formed

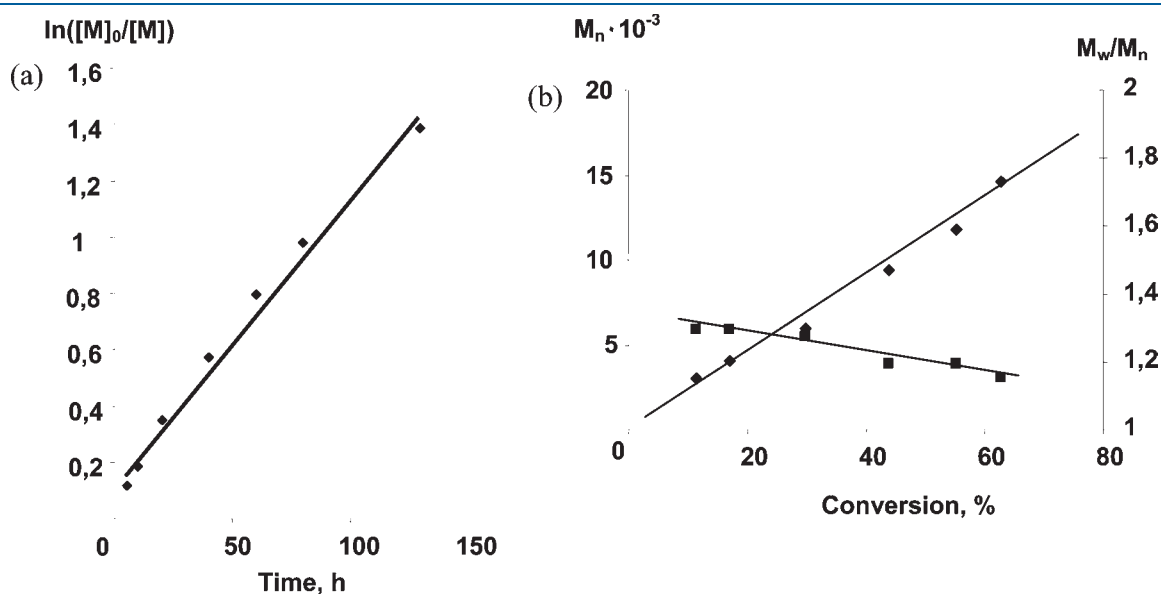


**Figure 9.** (a) First-order plot for monomer conversion versus time and (b) the dependence of  $M_n$  and  $M_w/M_n$  on conversion, for polymerization of MMA in the presence of 7 and  $\text{CCl}_4$ .



in situ from ruthenacarborane **3** during the polymerization of MMA, are the most probable catalyst precursors for the polymerization. It should be noted that on passing from **4** to species **5** a slight decrease in the polydispersity index was observed; i.e., the control of the polymerization over the chain growth step is enhanced in this case. Taking into account the higher stability of complex **5** under thermal conditions compared to other

compounds of this series, it can be speculated that this complex is the true precursor in the catalytic cycle of the controlled/living polymerization of MMA.

It should be noted that the molecular weights of the obtained samples are somewhat lower than those theoretically predicted from the initial ratio of MMA to initiator and conversion times. This fact may be due to the side processes that occur during the polymerization. The most significant difference between theoretically predicted and really achieved values is observed when complex **3** is used as the precatalyst, and this fact agreed well with an instability of **3** under the experimental conditions.

The dependence of MMA conversion versus time was investigated on complex **7**, as an example. The semilogarithmic plot of  $\ln([M]_0/[M]_t)$  versus time is linear (Figure 9a), indicating a constant concentration of active species during the polymerization and first-order kinetics with respect to monomer. Furthermore, the number-average molecular weight ( $M_n$ ) also increased linearly with conversion (Figure 9b) that indicates a constant number of polymer chains during the polymerization. These results suggest that radical polymerization with the catalyst **7** occurs in a controlled fashion. The same plots are observed for polymerization of MMA in the presence of two other complexes **4** and **5**.

**Table 4. Crystal Data and Details of the X-ray Experiments for Complexes 3 and 4**

	3	4
molecular formula	C <sub>30</sub> H <sub>40</sub> B <sub>9</sub> ClP <sub>2</sub> Ru	C <sub>30</sub> H <sub>39</sub> B <sub>9</sub> ClP <sub>2</sub> Ru · 0.3(C <sub>7</sub> H <sub>16</sub> ) · 0.2(C <sub>6</sub> H <sub>14</sub> )
fw	696.37	742.66
dimensions, mm <sup>3</sup>	0.36 × 0.33 × 0.16	0.26 × 0.12 × 0.08
cryst syst	monoclinic	monoclinic
space group	P2 <sub>1</sub> /n	C2/c
a, Å	12.4338(5)	12.4511(5)
b, Å	18.6092(7)	18.6812(7)
c, Å	14.7003(6)	30.6394(12)
α, deg		
β, deg	106.6710(10)	90.7650(10)
γ, deg		
V, Å <sup>3</sup>	3258.4(2)	7126.1(5)
Z	4	8
ρ <sub>calc</sub> g cm <sup>-3</sup>	1.420	1.384
2θ <sub>max</sub> deg	60	58
linear abs (μ), cm <sup>-1</sup>	6.83	6.30
no. unique reflns (R <sub>int</sub> )	9467 (0.0465)	9476 (0.0378)
no. obsd reflns (I > 2σ(I))	7591	7917
no. params	426	474
R1 (on F for obsd reflns) <sup>a</sup>	0.0332	0.0325
wR2 (on F <sup>2</sup> for all reflns) <sup>b</sup>	0.0793	0.0740
GOF	1.001	1.022

$${}^a R1 = \sum ||F_o| - |F_c|| / \sum |F_o|. \quad {}^b wR2 = \{ \sum [w(F_o^2 - F_c^2)^2] / \sum w(F_o^2)^2 \}^{1/2}.$$

## CONCLUSION

In this paper, the synthesis and structural characterization of a series of novel paramagnetic (17-electron) *closo*-ruthenacarboranes **4–7** have been described, some of which exhibit single or double *ortho*-cycloboronation of the ruthenium dppb ligand P-phenyl group. Formation of complex **7** featuring bis(*ortho*-cycloboronation) of the two phenyl groups bound to the same phosphorus atom of the dppb ligand is without precedent in

**Table 5. Crystal Data and Details of the X-ray Experiments for Complexes 5, 6, and 7**

	5	6	7
molecular formula	C <sub>30</sub> H <sub>37</sub> B <sub>9</sub> ClP <sub>2</sub> Ru · CH <sub>2</sub> Cl <sub>2</sub>	C <sub>30</sub> H <sub>36</sub> B <sub>9</sub> Cl <sub>2</sub> P <sub>2</sub> Ru	C <sub>30</sub> H <sub>35</sub> B <sub>9</sub> ClP <sub>2</sub> Ru
fw	778.27	727.79	691.33
dimensions, mm <sup>3</sup>	0.45 × 0.35 × 0.08	0.55 × 0.10 × 0.02	0.28 × 0.16 × 0.08
cryst syst	orthorhombic	triclinic	orthorhombic
space group	Pbca	P $\bar{1}$	Pbca
a, Å	17.2584(9)	10.332(2)	17.9940(11)
b, Å	14.1124(7)	10.450(2)	18.5256(11)
c, Å	28.7848(14)	16.281(3)	36.676(2)
α, deg		74.691(3)	
β, deg		76.727(3)	
γ, deg		82.264(3)	
V, Å <sup>3</sup>	7010.8(6)	1645.1(5)	12226.1(13)
Z	8	2	16
ρ <sub>calc</sub> g cm <sup>-3</sup>	1.475	1.469	1.502
2θ <sub>max</sub> deg	58	56	58
linear abs (μ), cm <sup>-1</sup>	7.91	7.59	7.28
no. unique reflns (R <sub>int</sub> )	9277 (0.0568)	7864 (0.0586)	16210 (0.1134)
no. obsd reflns (I > 2σ(I))	7511	5776	10712
no. params	455	397	775
R1 (on F for obsd reflns) <sup>a</sup>	0.0383	0.0416	0.0447
wR2 (on F <sup>2</sup> for all reflns) <sup>b</sup>	0.1022	0.0831	0.0998
GOF	1.040	0.994	1.023

$${}^a R1 = \sum ||F_o| - |F_c|| / \sum |F_o|. \quad {}^b wR2 = \{ \sum [w(F_o^2 - F_c^2)^2] / \sum w(F_o^2)^2 \}^{1/2}.$$

metallacarborane chemistry. The paramagnetic *closo*-ruthenacarborane complexes **4**, **5**, and **7** efficiently catalyzed the atom transfer radical polymerization of methyl methacrylate, affording MMA-based polymers with an extremely narrow molecular-weight distribution.

## EXPERIMENTAL SECTION

**General Considerations.** All thermal reactions were carried out in Schlenk equipment under an atmosphere of dry argon using standard Schlenk-line techniques. All solvents including those used as eluents for chromatography were distilled from appropriate drying agents under argon prior to use. Starting complex **3**<sup>5</sup> was prepared according to the published method. The EPR spectra were recorded in frozen toluene/CH<sub>2</sub>Cl<sub>2</sub> (1:1) mixture at 150 K with a Bruker-EMX spectrometer, operating at 9.75 GHz. IR spectra were obtained from KBr pellets on a Specord M-82 instrument. The EPR spectra were calibrated with diphenylpicrylhydrazyl (DPPH,  $g = 2.0037$ ). The HPLC used for analysis of ruthenacarborane mixtures formed in the reactions was performed on a Separon SGX column (150 mm in length and 3 mm in diameter, silica gel 5  $\mu$ ). The bulk polymerizations of MMA were performed in glass tubes under a residual pressure of monomer (1.3 Pa). The MWDs of the polymer samples were determined by SEC. All calculations were performed with Gaussian03<sup>19</sup> at the DFT (B3PW91<sup>20</sup> or B3LYP<sup>21</sup>) level. The optimizations, vibration frequency, and zero-point energy calculations were performed using the 6-31G(d) basis set for all atoms except for ruthenium, which is treated with Lanl2DZ with ECP.<sup>22</sup> Microanalyses were performed by the Analytical Laboratory of the Institute of Organoelement Compounds of the RAS.

**Thermal Transformation of Diamagnetic Complex [3,3-(dppb)-3-H-3-Cl-*closo*-3,1,2-RuC<sub>2</sub>B<sub>9</sub>H<sub>11</sub>] (**3**) in the presence of CCl<sub>4</sub>: Preparation of Paramagnetic Complex [3,3-(dppb)-3-Cl-*closo*-3,1,2-RuC<sub>2</sub>B<sub>9</sub>H<sub>11</sub>] (**4**).** To a stirred solution of freshly recrystallized **3** (100 mg, 0.14 mmol) in 20 mL of benzene was added 0.1 mL of degassed CCl<sub>4</sub> via syringe, and the resulting mixture was stirred at room temperature for 15 min, and then gently refluxed for ca. 4 h until starting complex **3** disappeared from the reaction mixture (HPLC control). After cooling, the solvent was evaporated under reduced pressure, and the residue was treated by column chromatography on silica gel. The first dark-red band eluted from the column with a benzene/*n*-hexane (2:1) mixture was found to contain the crude mixture of **4** and **5** in the approximate ratio 5:1, respectively (HPLC data). The second dark-red band contains traces (1.4 mg) of crude product **6**. After the evaporation of the solvent, the mixture of complexes **4** and **5** (79.2 mg) was repeatedly (3 times) recrystallized from CH<sub>2</sub>Cl<sub>2</sub> by addition of petroleum ether (bp 60–100 °C) followed by keeping the resulting dark red solution at +10 °C for 12 h. This resulted in isolation of 21 mg of **4** that contains, based on the HPLC data, less than 9.5% of **5**. Recrystallization of the residual obtained from the combined mother liquors afforded additionally up to 12 mg of pure complex **4** (total yield of **4** is ca. 34%). IR (KBr, cm<sup>-1</sup>): 2560 ( $\nu_{B-H}$ ). EPR (CH<sub>2</sub>Cl<sub>2</sub>/toluene, 150 K):  $g_1 = 2.487$ ;  $g_2 = 2.070$ ,  $g_3 = 1.947$ . Anal. Calcd for C<sub>30</sub>H<sub>39</sub>B<sub>9</sub>CIP<sub>2</sub>Ru·0.3*n*-C<sub>7</sub>H<sub>16</sub>: C, 53.15; H, 6.04; B, 13.41; P, 8.55. Found: C, 52.50; H, 6.26; B, 13.09; P, 8.24.

**Preparation of Paramagnetic Complex [3-Cl-3,3,8-{Ph<sub>2</sub>P-(CH<sub>2</sub>)<sub>4</sub>PPh- $\mu$ -(C<sub>6</sub>H<sub>4</sub>-*ortho*)}-*closo*-3,1,2-RuC<sub>2</sub>B<sub>9</sub>H<sub>10</sub>] (**5**) by the Mild Thermolysis of **3** and **4**.** Freshly prepared complex **3** (50 mg, 0.07 mmol) was dissolved in 15 mL of toluene, and the resulting yellow solution was stirred at 95 °C for 7 h. After cooling, the solvent was evaporated under vacuum, and the residue was purified using a short silica gel column (ca. 15–18 cm in length and 1.5 cm in diameter). The narrow dark-red band eluting with a benzene/*n*-hexane (2:1) mixture was collected and dried under vacuo. Recrystallization from

CH<sub>2</sub>Cl<sub>2</sub>/*n*-hexane at +5 °C for 12 h yielded 32 mg (64%) of the cherry-colored crystals, which from analysis of EPR spectrum and X-ray diffraction data is deduced to be paramagnetic complex **5**. IR (KBr, cm<sup>-1</sup>): 2562 ( $\nu_{B-H}$ ). EPR (CH<sub>2</sub>Cl<sub>2</sub>/toluene, 150 K):  $g_1 = 2.385$ ,  $g_2 = 2.095$ ,  $g_3 = 1.972$ . Anal. Calcd for C<sub>30</sub>H<sub>37</sub>B<sub>9</sub>CIP<sub>2</sub>Ru·0.5CH<sub>2</sub>Cl<sub>2</sub>: C, 49.79; H, 5.21; B, 13.22; P, 8.42. Found: C, 49.77; H, 5.51; B, 12.96; P, 7.99. An alternative route to **5** consisted of thermal treatment of **4** in toluene at 95 °C. Complex **4** (70 mg, 0.1 mmol), taken as a mixture of **4** and **5** in a ratio of ca. 4:1 (HPLC data), was stirred in toluene (15 mL) at 95 °C for 7.5 h. The solvent was evaporated under vacuum, and the residue was purified by column chromatography on silica gel similar to that described above. After isolation, the solid was recrystallized from CH<sub>2</sub>Cl<sub>2</sub> by addition of *n*-hexane, yielding 32.6 mg (47%) of the cherry-colored crystals, which from the comparative analysis of its HPLC data is deduced to be compound **5**.

### Preparation of Paramagnetic Complex [3-Cl-3,3,7,8-

{Ph<sub>2</sub>P(CH<sub>2</sub>)<sub>4</sub>P- $\mu$ -(C<sub>6</sub>H<sub>4</sub>-*ortho*)<sub>2</sub>}-*closo*-3,1,2-RuC<sub>2</sub>B<sub>9</sub>H<sub>9</sub>] (**7**) by Thermolysis of **3** and **5**.

A stirred solution of freshly prepared **3** (340 mg, 0.49 mmol) in 15 mL of toluene was gently refluxed for 5 h under argon atmosphere. The solvent was concentrated to dryness under reduced pressure, and the residue was treated by column chromatography on silica gel. The first dark-red band obtained from the column using a benzene/*n*-hexane (2:1) mixture was then purified by recrystallization from CH<sub>2</sub>Cl<sub>2</sub>/*n*-hexane to give 66 mg (19.5%) of dark-red crystals, which from analysis of EPR spectrum is deduced to be paramagnetic complex **5**. The second band was then eluted with benzene to afford, after the evaporation of the solvent and recrystallization of the crude material from CH<sub>2</sub>Cl<sub>2</sub>/*n*-hexane, analytically pure **7** (41 mg, 12%) as olive-brown crystals. Data for **7** follow. IR (KBr, cm<sup>-1</sup>): 2555 ( $\nu_{B-H}$ ). EPR (CH<sub>2</sub>Cl<sub>2</sub>/toluene, 150 K):  $g_1 = 2.300$ ,  $g_2 = 2.091$ ,  $g_3 = 1.986$ . Anal. Calcd for C<sub>30</sub>H<sub>35</sub>B<sub>9</sub>CIP<sub>2</sub>Ru: C, 52.12; H, 5.10; B, 14.07; P, 8.96. Found: C, 51.79; H, 5.13; B, 13.93; P, 8.76. An alternative route to **7** consisted of thermal reaction of **5** in toluene at reflux. A solution of freshly prepared **5** (60 mg, 0.09 mmol) in 15 mL of toluene was gently refluxed with stirring for 14 h under argon. The solution was cooled to ambient temperature, and the toluene was evaporated under reduced pressure. The resulting solid was then treated by column chromatography on silica gel using a mixture of benzene/*n*-hexane (2:1) as eluent. The first dark-red band eluted from the column was found to contain crude starting complex **5**, which was then recrystallized from CH<sub>2</sub>Cl<sub>2</sub>/*n*-hexane, yielding 19 mg (32%) of pure **5** as dark-red crystals. The second fraction eluted with benzene was collected and dried under vacuum, affording 22 mg of **7** as a brown crystalline solid (37% yield).

### Preparation of Paramagnetic Complex [3,7-Cl<sub>2</sub>-3,3,8-

{Ph<sub>2</sub>P(CH<sub>2</sub>)<sub>4</sub>PPh- $\mu$ -(C<sub>6</sub>H<sub>4</sub>-*ortho*)}-*closo*-3,1,2-RuC<sub>2</sub>B<sub>9</sub>H<sub>10</sub>] (**6**) by Heating of **5** in CCl<sub>4</sub>.

A stirred solution of 33 mg (0.048 mmol) of **5** in 15 mL of CCl<sub>4</sub> was gently refluxed for 20.5 h. Chlorinated solvent was removed in vacuum, and the residue was purified by column chromatography on silica gel using CH<sub>2</sub>Cl<sub>2</sub>/*n*-hexane (2:1) mixture as eluent. The solvent was evaporated under reduced pressure, and the crude solid material was recrystallized from CH<sub>2</sub>Cl<sub>2</sub>/*n*-hexane affording complex **6** (23 mg, 68%) as ruby crystals. Data for **6** follow. IR (KBr, cm<sup>-1</sup>): 2580 ( $\nu_{B-H}$ ). EPR (CH<sub>2</sub>Cl<sub>2</sub>/toluene, 150 K):  $g_1 = 2.384$ ,  $g_2 = 2.091$ ,  $g_3 = 1.965$ . Anal. Calcd for C<sub>30</sub>H<sub>36</sub>B<sub>9</sub>CIP<sub>2</sub>Ru: C, 49.51; H, 4.98; Cl, 9.74. Found: C, 49.83; H, 4.66; Cl, 9.69.

**Polymerization Procedure.** A typical experiment of the MMA polymerization with complex **3** is given as example below. In a glass tube was placed complex **3** (6.9 mg, 0.01 mmol), solution of CCl<sub>4</sub> (0.2 mL of 0.1 M in toluene, 0.02 mmol), and MMA (0.8 mL, 7.6 mmol). The oxygen was removed via three freeze–pump–thaw cycles, and the tube was then sealed and placed in an oil bath with thermostat set at 80 °C. In predetermined time, the polymerization was terminated by cooling the

tube with the reaction mixture in liquid nitrogen. The polymer formed was diluted with  $\text{CHCl}_3$  (ca. 5 mL) and precipitated with an excess of *n*-hexane. This procedure was repeated one more time, and the polymer obtained was dried at 50 °C under vacuum to the constant weight. Monomer conversion was determined gravimetrically. All polymers obtained by this method were then analyzed by SEC on a Knauer instrument equipped with two polystyrene gel columns (Phenomenex, pore size  $10^3$ – $10^5$  Å) and an RI Detector K-2301 differential refractometer as the detector. THF was used as the eluent. The columns were calibrated against 8 standard poly(methyl methacrylate) samples received from Waters (the  $M_n$  varies from 2580 to  $9.81 \times 10^5$ ).

**X-ray Diffraction Studies of Complexes 3–7.** Single-crystal X-ray diffraction experiment in all cases was carried out with a Bruker SMART APEX II diffractometer (graphite monochromated Mo K $\alpha$  radiation,  $\lambda = 0.71073$  Å,  $\omega$ -scan technique,  $T = 100$  K). The APEX II software<sup>23</sup> was used for collecting frames of data, indexing reflections, determination of lattice constants, integration of intensities of reflections, scaling, and absorption correction, and SHELXTL<sup>24</sup> was used for space group and structure determination, refinements, graphics, and structure reporting. The structures were solved by direct methods and refined by the full-matrix least-squares technique against  $F^2$  with the anisotropic temperature factors for all non-hydrogen atoms. The hydrogen atoms of carborane moieties in structures 3–7 as well as the hydride ligand in complex 3 were located from difference Fourier maps and refined isotropically. The H(C) atoms were placed geometrically and included in the structure factors calculation in the riding motion approximation. The principal experimental and crystallographic parameters are presented in Tables 4 and 5.

## ■ ASSOCIATED CONTENT

**S Supporting Information.** CIF files giving X-ray crystallographic data for complexes 3, 4, 5, 6, and 7. Cartesian coordinates of all optimized structures with energies. This material is available free of charge via the Internet at <http://pubs.acs.org>.

## ■ AUTHOR INFORMATION

### Corresponding Author

\*E-mail: [chizbor@ineos.ac.ru](mailto:chizbor@ineos.ac.ru).

## ■ ACKNOWLEDGMENT

This work has been supported by Grants 09-03-00211, 10-03-00505, and 11-03-00074 from the Russian Foundation for Basic Research. The authors are also grateful to Dr. M. G. Ezernitskaya for recording IR spectra of complexes 3–7.

## ■ REFERENCES

- (1) (a) Kharasch, M. S.; Jensen, E. V.; Urry, W. H. *Science* **1945**, *102*, 128. (b) Kharasch, M. S.; Urry, W. H.; Jensen, E. V. *J. Am. Chem. Soc.* **1945**, *67*, 1626.
- (2) See for the latest reviews: (a) di Lena, F.; Matyjaszewski, K. *Prog. Polym. Sci.* **2010**, *35*, 959. (b) Ouchi, M.; Terashima, T.; Sawamoto, M. *Chem. Rev.* **2009**, *109*, 4963. (c) Grishin, I. D.; Grishin, D. F. *Russ. Chem. Rev.* **2008**, *77*, 633.
- (3) (a) Takahashi, H.; Ando, T.; Kamigaito, M.; Sawamoto, M. *Macromolecules* **1999**, *32*, 3820. (b) Ando, T.; Kamigaito, M.; Sawamoto, M. *Macromolecules* **2000**, *33*, 5825. (c) Watanabe, Y.; Ando, T.; Kamigaito, M.; Sawamoto, M. *Macromolecules* **2001**, *34*, 4370. (d) Tutusaus, O.; Delfosse, S.; Simal, F.; Demonceau, A.; Noels, A. F.; Nuñez, R.; Vinas, C.; Teixidor, F. *Inorg. Chem. Commun.* **2002**, 941. (e) Simal, F.; Demonceau, A.; Noels, A. F. *Angew. Chem., Int. Ed.* **1999**, *38*, 538. (f) Simal, F.; Jan, D.; Delaude, L.; Demonceau, A.; Spirlet, M.-R.

- (g) Noels, A. F. *Can. J. Chem.* **2001**, *79*, 529. (g) Delaude, L.; Delfosse, S.; Richel, A.; Demonceau, A.; Noels, A. F. *Chem. Commun.* **2003**, 1526. (h) Richel, A.; Delfosse, S.; Cremasco, C.; Delaude, L.; Demonceau, A.; Noels, A. F. *Tetrahedron Lett.* **2003**, *44*, 6011. (i) Borguet, Y.; Sauvage, X.; Bicchielli, D.; Delfosse, S.; Delaude, L.; Demonceau, A.; Bareille, L. *Controlled/Living Radical Polymerization: Progress in ATRP*; ACS Symposium Series; American Chemical Society: Washington, DC, 2009; Vol. 1023, Chapter 7, p 97. (j) Kato, M.; Kamigaito, M.; Sawamoto, M.; Higashimura, T. *Macromolecules* **1995**, *28*, 1721. (k) Ando, T.; Kato, M.; Kamigaito, M.; Sawamoto, M. *Macromolecules* **1996**, *29*, 1070. (l) Simal, F.; Demonceau, A.; Noels, A. F. *Tetrahedron Lett.* **1999**, *40*, 5689. (m) Simal, F.; Sebille, S.; Demonceau, A.; Noels, A. F.; Nuñez, R.; Abad, M.; Teixidor, F.; Vinas, C. *Tetrahedron Lett.* **2000**, *41*, 5347. (n) Tutusaus, O.; Nuñez, R.; Vinas, C.; Teixidor, F.; Mata, I.; Molins, E. *Inorg. Chem.* **2004**, *43*, 6067.

- (4) (a) Hawthorne, M. F. *Acc. Chem. Res.* **1968**, *1*, 281. (b) Callahan, K. P.; Hawthorne, M. F. *Adv. Organomet. Chem.* **1976**, 145. (c) Hanusa, T. P. *Polyhedron* **1982**, *1*, 663. (d) Warren, L. F.; Hawthorne, M. F. *J. Am. Chem. Soc.* **1970**, *92*, 1157. (e) Clair, D. S.; Zalkin, A.; Templeton, D. H. *J. Am. Chem. Soc.* **1970**, *92*, 1173.

- (5) (a) Wong, E. H. S.; Hawthorne, M. F. *J. Chem. Soc., Chem. Commun.* **1976**, 257. (b) Wong, E. H. S.; Hawthorne, M. F. *Inorg. Chem.* **1978**, *17*, 2863. (c) Chizhevsky, I. T.; Lobanova, I. A.; Bregadze, V. I.; Petrovskii, P. V.; Polyakov, A. V.; Yanovsky, A. I.; Struchkov, Yu. T. *Organomet. Chem. USSR (Engl. Transl.)* **1991**, *4*, 469. (d) Cheredilin, D. N.; Dolgushin, F. M.; Grishin, I. D.; Kolyakina, E. V.; Nikiforov, A. S.; Solodovnikov, S. P.; Il'in, M. M.; Davankov, V. A.; Chizhevsky, I. T.; Grishin, D. F. *Russ. Chem. Bull.* **2006**, *55*, 1163. (e) Ellis, D. D.; Couchman, S. M.; Jeffery, J. C.; Malget, J. M.; Stone, F. G. A. *Inorg. Chem.* **1999**, *38*, 2981.

- (6) Cheredilin, D. N.; Balagurova, E. V.; Godovikov, I. A.; Solodovnikov, S. P.; Chizhevsky, I. T. *Russ. Chem. Bull.* **2005**, *54*, 2535.

- (7) (a) Kolyakina, E. V.; Grishin, I. D.; Cheredilin, D. N.; Dolgushin, F. M.; Chizhevsky, I. T.; Grishin, D. F. *Russ. Chem. Bull.* **2006**, *55*, 89. (b) Grishin, I. D.; Kolyakina, E. V.; Cheredilin, D. N.; Chizhevsky, I. T.; Grishin, D. F. *Polym. Sci. A* **2007**, *49*, 1079. (c) Grishin, I. D.; Chizhevsky, I. T.; Grishin, D. F. *Dokl. Chem.* **2008**, *423*, 290. (d) Grishin, I. D.; Chizhevsky, I. T.; Grishin, D. F. *Kinet. Catal.* **2009**, *50*, 550. (e) Grishin, D. F.; Grishin, I. D.; Chizhevsky, I. T. *Controlled/Living Radical Polymerization: Progress in ATRP*; ACS Symposium Series; American Chemical Society: Washington, DC, 2009; Vol. 1023, Chapter 8, p 115.

- (8) Grishin, I. D.; D'iachikhin, D. I.; Dolgushin, F. M.; Grishin, D. F.; Chizhevsky, I. T. *Abstracts of the Fifth European Meeting on Boron Chemistry (EUROBORON 5)*; Heriot-Watt University, Edinburgh, U.K., August 29–September 2, 2010; Abstract no. O 18, p 39.

- (9) (a) Crook, J. E.; Greenwood, N. N.; Kennedy, J. D.; McDonald, W. S. *J. Chem. Soc., Chem. Commun.* **1981**, 933. (b) Kukina, G. A.; Sergienko, V. S.; Porai-Koshits, M. A. *Koord. Khim.* **1985**, *11*, 400. (c) McGrath, T. D.; Franken, A.; Kautz, J. A.; Stone, F. G. A. *Inorg. Chem.* **2005**, *44*, 8135.

- (10) Cheredilin, D. N.; Kadyrov, R.; Dolgushin, F. M.; Balagurova, E. V.; Godovikov, I. A.; Solodovnikov, S. P.; Chizhevsky, I. T. *Inorg. Chem. Commun.* **2005**, *8*, 614.

- (11) (a) Bould, J.; Crook, J. E.; Greenwood, N. N.; Kennedy, J. D.; McDonald, W. S. *J. Chem. Soc., Chem. Commun.* **1982**, 465. (b) Bould, J.; Crook, J. E.; Greenwood, N. N.; Kennedy, J. D.; McDonald, W. S. *J. Chem. Soc., Chem. Commun.* **1983**, 949. (c) Elrinton, M.; Greenwood, N. N.; Kennedy, J. D.; Thornton-Pett, M. *J. Chem. Soc., Dalton Trans.* **1986**, 2277. (d) Ferguson, G.; Jennings, M. C.; Lough, A. J.; Loughlan, S.; Spalding, T. R.; Kennedy, J. D.; Fontain, X. R. *J. Chem. Soc., Chem. Commun.* **1990**, 891. (e) Bould, J.; Greenwood, N. N.; Kennedy, J. D. *J. Chem. Soc., Dalton Trans.* **1990**, 1451. (f) Bould, J.; Brint, P.; Kennedy, J. D.; Thornton-Pett, M. *J. Chem. Soc., Dalton Trans.* **1993**, 2335. (g) Dou, J.-M.; Hu, C.-H.; Li, W.; Yao, H.-J.; Jin, R.-S.; Zheng, P.-J. *Polyhedron* **1997**, *16*, 2323. (h) Bould, J.; Clegg, W.; Teat, S. J.; Barton, L.; Rath, N. P.; Thornton-Pett, M.; Kennedy, J. D. *Inorg. Chim. Acta* **1999**, *289*, 95.

- (12) (a) Lahiri, G. K.; Bhattacharya, S.; Mukherjee, M.; Mukherjee, A. K.; Chakravorty, A. *Inorg. Chem.* **1987**, *26*, 3359. (b) Munshi, P.; Samanta, R.; Lahiri, G. K. *J. Organomet. Chem.* **1999**, *586*, 176.

(13) Pisareva, I. V.; Dolgushin, F. M.; Tok, O. L.; Konoplev, V. E.; Suponitsky, K. Yu.; Yanovsky, A. I.; Chizhevsky, I. T. *Organometallics* **2001**, *20*, 4116.

(14) Chizhevsky, I. T.; Lobanova, I. A.; Petrovskii, P. V.; Bregadze, V. I.; Dolgushin, F. M.; Yanovsky, A. I.; Struchkov, Yu. T.; Chistyakov, A. L.; Stankevich, I. V.; Knobler, C. B.; Hawthorne, M. F. *Organometallics* **1999**, *18*, 726.

(15) Anderson, S.; Mullica, D. F.; Sappenfield, E. L.; Stone, F. G. A. *Organometallics* **1995**, *14*, 3516.

(16) (a) Baše, K.; Petřina, A.; Štíbr, B.; Kukina, G. A.; Zakharova, I. A. *Proc. 8th Conf. Coord. Chem. (Czechoslovakia)* **1980**, *17*. *Chem. Abstr.* **1981**, *95*, 23933g.

(17) (a) Crook, J. E.; Greenwood, N. N.; Kennedy, J. D.; McDonald, W. S. *J. Chem. Soc., Chem. Commun.* **1982**, 383.

(18) (a) Braunecker, W.; Brown, W.; Morelli, B.; Tang, W.; Poli, R.; Matyjaszewski, K. *Macromolecules* **2007**, *40*, 8576. (b) Comas-Vives, A.; Ujaque, G.; Lledós, A. *Organometallics* **2008**, *27*, 4854. (c) Mathew, J.; Koga, N.; Suresh, C. H. *Organometallics* **2008**, *27*, 4666. (d) Ayed, T.; Barthelat, J.-C.; Tangour, B.; Pradère, C.; Donnadieu, B.; Grellier, M.; Sabo-Etienne, S. *Organometallics* **2005**, *24*, 3824. (e) Rose, M. J.; Mascharak, P. K. *Inorg. Chem.* **2009**, *48*, 6904.

(19) Frisch, M. J.; Trucks, G. W.; Schlegel, H. B.; Scuseria, G. E.; Robb, M. A.; Cheeseman, J. R.; Montgomery, J. A., Jr.; Vreven, T.; Kudin, K. N.; Burant, J. C.; Millam, J. M.; Iyengar, S. S.; Tomasi, J.; Barone, V.; Mennucci, B.; Cossi, M.; Scalmani, G.; Rega, N.; Petersson, G. A.; Nakatsuji, H.; Hada, M.; Ehara, M.; Toyota, K.; Fukuda, R.; Hasegawa, J.; Ishida, M.; Nakajima, T.; Honda, Y.; Kitao, O.; Nakai, H.; Klene, M.; Li, X.; Knox, J. E.; Hratchian, H. P.; Cross, J. B.; Bakken, V.; Adamo, C.; Jaramillo, J.; Gomperts, R.; Stratmann, R. E.; Yazyev, O.; Austin, A. J.; Cammi, R.; Pomelli, C.; Ochterski, J. W.; Ayala, P. Y.; Morokuma, K.; Voth, G. A.; Salvador, P.; Dannenberg, J. J.; Zakrzewski, V. G.; Dapprich, S.; Daniels, A. D.; Strain, M. C.; Farkas, O.; Malick, D. K.; Rabuck, A. D.; Raghavachari, K.; Foresman, J. B.; Ortiz, J. V.; Cui, Q.; Baboul, A. G.; Clifford, S.; Cioslowski, J.; Stefanov, B. B.; Liu, G.; Liashenko, A.; Piskorz, P.; Komaromi, I.; Martin, R. L.; Fox, D. J.; Keith, T.; Al-Laham, M. A.; Peng, C. Y.; Nanayakkara, A.; Challacombe, M.; Gill, P. M. W.; Johnson, B.; Chen, W.; Wong, M. W.; Gonzalez, C.; Pople, J. A. *Gaussian 03, Revision E.01*; Gaussian, Inc.: Wallingford, CT, 2004.

(20) Perdew, J. P.; Wang, Y. *Phys. Rev. B* **1992**, *45*, 13244.

(21) (a) Becke, A. D. *J. Chem. Phys.* **1993**, *98*, 5648. (b) Lee, C.; Yang, W.; Parr, R. G. *Phys. Rev. B* **1988**, *37*, 785.

(22) Hay, P. J.; Wadt, W. R. *J. Chem. Phys.* **1985**, *82*, 270.

(23) *APEX II Software Package*; Bruker AXS Inc.: Madison, WI, 2005.

(24) Sheldrick, G. M. *Acta Crystallogr.* **2008**, *A64*, 112.